



# A brush-coating approach to achieve anisotropic optical film via field-induced stretching of carbon nanotube clusters in a reactive mesogen

Cite as: AIP Advances 10, 095308 (2020); <https://doi.org/10.1063/5.0018481>

Submitted: 15 June 2020 . Accepted: 21 August 2020 . Published Online: 08 September 2020

Young Jin Lim, Ramesh Manda , Kyung Jun Cho, Tae Hyung Kim, Weiwei Tie, Jorge Torres, Minhee Yun, and Seung Hee Lee 

## COLLECTIONS

Paper published as part of the special topic on [Chemical Physics](#), [Energy](#), [Fluids and Plasmas](#), [Materials Science](#) and [Mathematical Physics](#)



View Online



Export Citation



CrossMark



**NEW!**

Sign up for topic alerts  
New articles delivered to your inbox



# A brush-coating approach to achieve anisotropic optical film via field-induced stretching of carbon nanotube clusters in a reactive mesogen

Cite as: AIP Advances 10, 095308 (2020); doi: 10.1063/5.0018481

Submitted: 15 June 2020 • Accepted: 21 August 2020 •

Published Online: 8 September 2020



View Online



Export Citation



CrossMark

Young Jin Lim,<sup>1</sup> Ramesh Manda,<sup>1</sup>  Kyung Jun Cho,<sup>1</sup> Tae Hyung Kim,<sup>1</sup> Weiwei Tie,<sup>2,3,a)</sup> Jorge Torres,<sup>4</sup> Minhee Yun,<sup>4</sup> and Seung Hee Lee<sup>1,a)</sup> 

## AFFILIATIONS

<sup>1</sup>Department of Nanoconvergence Engineering Department of Polymer Nano Science and Technology, Jeonbuk National University, Jeonju, Jeonbuk 54896, South Korea

<sup>2</sup>Key Laboratory of Micro-Nano Materials for Energy Storage and Conversion of Henan Province, School of Advanced Materials and Energy, Institute of Surface Micro and Nanomaterials, Xuchang University, Xuchang, Henan 461000, China

<sup>3</sup>Henan Joint International Research Laboratory of Nanomaterials for Energy and Catalysis, Xuchang University, Xuchang, Henan 461000, China

<sup>4</sup>Department of Electrical and Computer Engineering, Swanson School of Engineering, University of Pittsburgh, Pittsburgh, Pennsylvania 15261, USA

<sup>a)</sup> Authors to whom correspondence should be addressed: [tieweiwei@xcn.edu.cn](mailto:tieweiwei@xcn.edu.cn) and [lsh1@jbnu.ac.kr](mailto:lsh1@jbnu.ac.kr)

## ABSTRACT

We present a novel brush coating method for fabricating a coatable polarizer that utilizes a mixture of functionalized single-walled carbon nanotubes (h-SWCNTs) grafted with carboxyl and hydroxyl groups and a reactive mesogen (RM), which possess a long-range orientational ordering of their rod-shaped molecules with photo-sensitive functional groups. The h-SWCNTs are shortened to a length of around 150 nm by an acid sonochemical oxidation process and then dispersed in an RM solution. The brush-coated thin layer initially consists of h-SWCNT clusters, but applying an in-plane electric field induces large-scale stretching of these along the field direction, after which the layer is photo-polymerized by ultraviolet irradiation to form a film embedding the stretched nanotubes. The uniaxially aligned carbon nanotubes (CNTs) produce a broadband absorption spectrum that enables the film to exhibit an optical anisotropic property that absorbs incident light from the ultraviolet to the visible spectrum selectively depending on the polarization direction, thus acting as a coatable CNT polarizer. The dispersibility and elongation of h-SWCNT clusters induced by applying the electric field, as well as the anisotropic light-absorption properties of the h-SWCNT film, are investigated.

© 2020 Author(s). All article content, except where otherwise noted, is licensed under a Creative Commons Attribution (CC BY) license (<http://creativecommons.org/licenses/by/4.0/>). <https://doi.org/10.1063/5.0018481>

## I. INTRODUCTION

A polarizer is now one of the indispensable materials in liquid crystal displays and organic light-emitting diode displays. A conventional polarizer is made of stretched polyvinyl alcohol (PVA) with embedded iodine ions; hence, protection films are required on both sides of the PVA film.<sup>1</sup> Tri-acetyl cellulose films are widely used

as protection films that usually provide zero retardation. However, due to the multi-layered structure of protection films, the polarizer becomes bulky (>50 μm), which restricts its application to flexible display devices. Furthermore, the recent development of flexible displays requires novel polarizers that can maintain a higher flexibility.<sup>2,3</sup> Recently, a coatable polarizer based on lyotropic chromonic (LC),<sup>4-6</sup> photoaligned LC,<sup>7-9</sup> and dichroic dye incorporated LC



mixtures<sup>10–12</sup> has been proposed, which can overcome these disadvantages. Owing to its ultra-thin thickness of only a few micrometers, this film is easily adaptable to any plastic/flexible substrate utilized for display devices, including bendable and foldable, roll-to-roll, rugged, or stretchable displays. One of the primary advantages of coatable polarizers lies in the fact that they are tunable in response to external stimuli. However, their performance is severely deteriorated by lowered thermal stability due to involvement of organic materials.

Recently, uniformly-aligned carbon nanotubes (CNTs) have been recognized as a viable alternative to flexible polarizers owing to their anisotropic optical absorption.<sup>13–15</sup> Since one of the intrinsic properties of CNTs is their  $\pi$  plasmon-originated broad absorption spectrum, uniformly-aligned CNTs can act as an efficient polarizer not only for the visible region but also for the ultraviolet (UV) region.<sup>13</sup> Our group has previously reported a coatable thin-film polarizer based on functionalized CNT clusters/reactive mesogen (RM) mixtures, in which the CNT clusters are stretched and unidirectionally oriented by an external stimulus such as an electric field.<sup>16</sup> While an incident light with its polarization axis perpendicular to the long axis of the stretched clusters is transmitted through them, the light with its polarization axis parallel to the long axis of the stretched clusters is blocked by them. Thanks to remarkable improvements in the thermal stability and high conductivity of CNTs over iodine and selective light absorption of stretched CNT clusters, this approach can extend their applications to many other areas, from broadband polarizers to more thermal-resistant and less electrostatic polarizers. This method also offers the advantage of large-scale film manufacturing. Despite their many potential applications, the conventional approach to obtain a thin film of an LC/CNT composite by spin coating results in a huge CNT agglomeration in which the field-induced orientation is very difficult. In addition, the low polarization efficiency of CNT polarizers remains a critical challenge due to the difficulty in achieving large-scale orientation ordering of CNT rods. It is required to develop a robust method to improve the degree of orientation of CNT rods on a large-scale.

In this work, we present a brush-coating method for improving the polarization efficiency of CNT polarizers in large spaces between electrodes, by enhancing the orientation of functionalized single-walled CNTs (SWCNTs). The functionalized SWCNT clusters are stretched in an RM medium along the field direction by an applied electric field. CNT orientation ordering is maintained with an external electric field as well as the liquid crystal direction field of RM molecules, while RM polymerization by UV exposure fixes the CNT alignment. The proposed CNT polarizer has an advantage of improved CNT alignment over a large area and a wide transmittance spectrum from UV to visible light, as well as being more cost-effective than CNT polarizers fabricated using the spin-coating method. Moreover, the ease of processing and uniform polarization properties of CNT polarizers not only make them potentially applicable to large-sized flexible displays but also open up new methods for developing such displays in the future.

## II. EXPERIMENT

An SWCNT sample with carboxyl group functionality was purchased from Avention, Inc. (AV-4122, South Korea). The purchased

pristine SWCNT sample was in a powder form. The average outer diameter of each SWCNT is  $\sim 2$  nm while the length varies from 1  $\mu\text{m}$  to 3  $\mu\text{m}$ . Acid sonochemical oxidation treatment was performed to modify the surface functionality and length of the SWCNTs.<sup>17</sup> In brief, 5 mg of pristine SWCNT was dispersed in a mixture solution of sulfuric acid (3 ml) and nitric acid (1.5 ml), and sonochemical treatment was performed by sonicating this mixture for 3 h at 60 °C using an ultrasonic bath (Mujigae, SD-D300H, 40 kHz frequency and 200 W output). Sonochemically treated SWCNTs were obtained after separation of the supernatant by centrifuging at 12 000 rpm for 25 min. The obtained sample was again thoroughly washed with deionized water to separate the leftover supernatant. Finally, the sample was oven-dried at 80 °C for 30 min, and the final powder was collected, which hereafter will be referred to as h-SWCNTs. The resulting h-SWCNT powder was dispersed in ethanol solution and stored at room temperature. The functionality and morphological analysis of synthesized h-SWCNTs were verified by Fourier transform infrared spectroscopy (FTIR) (Shimadzu, IRTracer-100) and using a field emission scanning electron microscope (FESEM) (Hitachi, SU-70), respectively.

The h-SWCNT with a known concentration of ethanol was added to an RM solution (RMS03-013C, from Merck, Germany) and magnetically stirred for 5 min. A small amount of photo-initiator, Irgacure-907, was added to this mixture in order to initiate the crosslinking polymerization of the RM. The homogeneous mixture of the h-SWCNT and RM was spin-coated or brush-coated onto a substrate consisting of interdigitated indium-tin-oxide electrodes (electrode width  $\times$  separation = 5  $\times$  75  $\mu\text{m}^2$ ). An electric field was then applied to the substrate to observe the field-induced stretching of the h-SWCNT. The ethanol solvent was evaporated by heating the substrate to 50 °C. The h-SWCNT concentration in the RM solution was around 2 wt. %.

A schematic of the fabrication process and the electric field-induced h-SWCNT stretching mechanism is shown in Fig. 1. Before applying the voltage, the direction of the SWCNT clusters in the RM solution initially tended to be random due to strong van der Waals interactions, as shown in Fig. 1(a). As an electric field was applied, however, both the RM and the SWCNT appeared to undergo a field-induced reorientation and stretching, along the direction of the electric field. When an electric field is applied, a strong dielectric coupling between the RM and the electric field aligned them along the field direction. In the same way, the charge localization and dielectrophoresis torque induced under a strong electric field are believed to stretch the SWCNT cluster along the field direction.<sup>19</sup> The interaction between the RM and the SWCNT can be assumed to be the same as that for the LC and the SWCNT. In this position, UV irradiation (LC8, Lighting cure, Hamamatsu, 365 nm emission band) with 25 mW/cm<sup>2</sup> intensity was performed for 120 s to polymerize the RM which in turn fixes the stretching direction of the SWCNT, as shown in Fig. 1(b). After UV irradiation, the electric field was withdrawn, and a stable LC polymer film with unidirectionally oriented h-SWCNTs was realized, as shown in Fig. 1(c). The wavelength-dependent characteristics were observed by the UV-visible spectroscopy (Scinco, S-3100). A polarizer was connected where polarized light is required. The polarization efficiency of the synthesized polarizers was estimated by rotating one of the two polarizers fixed above another of the same type. After passing through the two polarizers, the relative transmittance of incident white light was



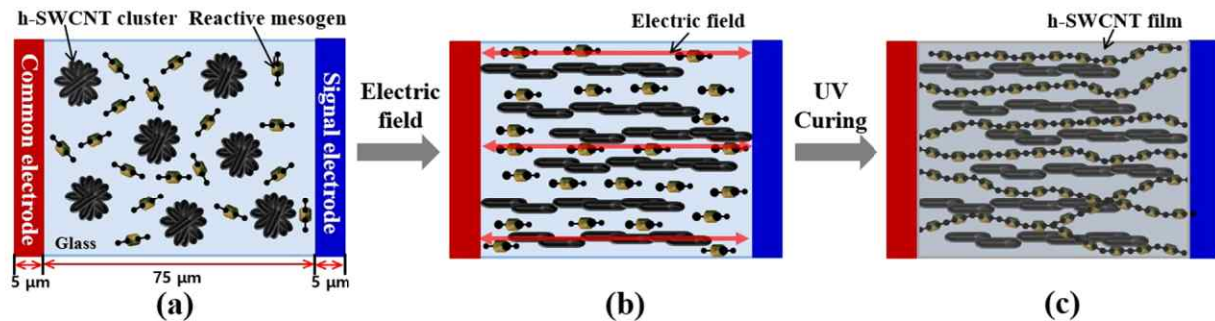


**FIG. 1.** Schematic of the processing steps for fabricating electric field-induced stretching of h-SWCNT clusters in an RM solution: (a) coating an h-SWCNT and RM mixture on the substrate with interdigitated electrodes, (b) electric field induced RM orientation and substantial orientation and stretching of h-SWCNT clusters along the field direction followed by stabilization of the film by using a UV irradiation, and (c) liquid crystal polymer film with aligned h-SWCNTs after withdrawn electric field.

detected by a photodiode at different rotation angles of the lower polarizer.

### III. RESULTS AND DISCUSSION

Our analysis begins with the functionality and morphological characterization of synthesized SWCNTs using an FTIR and FESEM. The FESEM images of the SWCNT before and after sonochemical treatment were used for morphological analysis. Figures 2(a) and 2(b) show the FESEM micrograph of the SWCNT before and after sonochemical treatment. The average length of the SWCNTs was reduced to 150 nm after sonochemical treatment

[calculated from the center wavelength of Gaussian distribution, Fig. 2(c)]. The surface functionality of the h-SWCNTs was characterized by comparing the *in situ* FTIR spectra of SWCNTs that were achieved before and after sonochemical treatment. The FTIR spectra shown in Fig. 2(d) exhibit peaks at  $3362\text{ cm}^{-1}$  (—OH— stretching),  $2917\text{ cm}^{-1}$  (—CH<sub>2</sub>— stretching),  $1711\text{ cm}^{-1}$  (—C=O— stretching in carboxylic acid),  $1578\text{ cm}^{-1}$  (conjugated —C=C— stretching of the carbon skeleton), and  $1174\text{ cm}^{-1}$  (—C—O— stretching in alcohol). The absorption bands at  $3362\text{ cm}^{-1}$  and  $1711\text{ cm}^{-1}$  are observed due to an increase in O—H stretching present in both the carboxylic acid and alcohol groups and C=O stretching in carboxylic acids, respectively. In particular, the new characteristic peak that appears

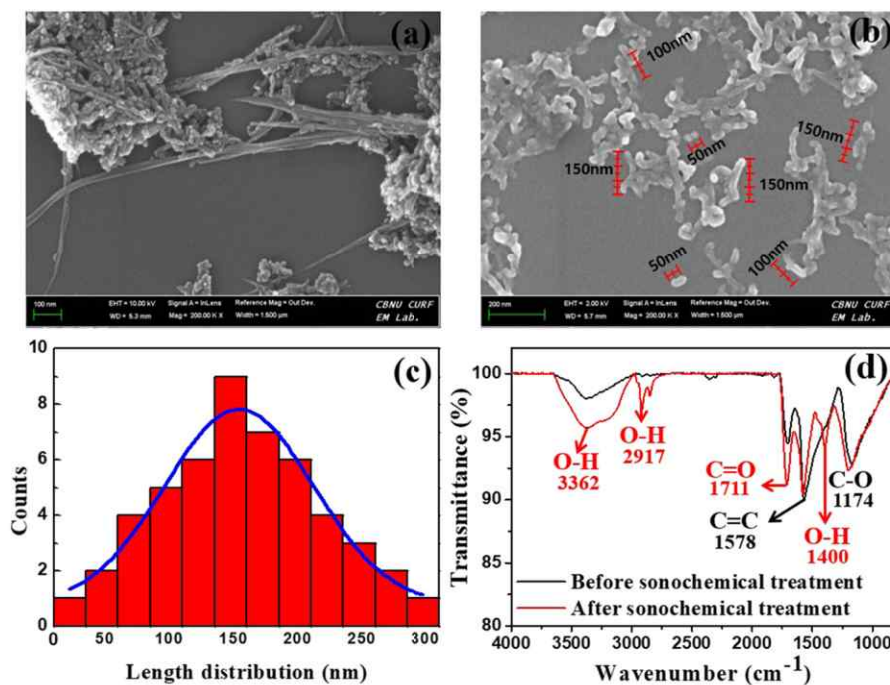


**FIG. 2.** FESEM images of the SWCNT (a) before and (b) after sonochemical treatment, (c) calculated h-SWCNT length distribution and corresponding Gaussian fit, and (d) FTIR spectra of the SWCNT before and after sonochemical treatment.



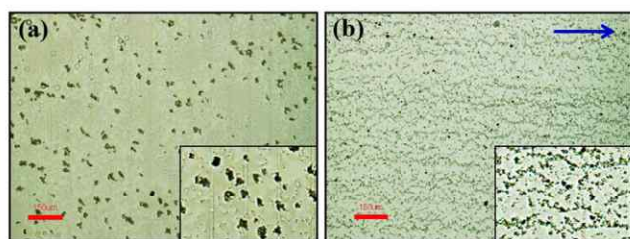


**FIG. 3.** Optical microscopy images of fabricated h-SWCNT films using (a) spin-coating and (b) brush-coating methods before UV irradiation. The blue arrow indicates the brushing direction.

at  $1400\text{ cm}^{-1}$  may have originated from the O–H bonding of the aliphatic group that was grafted onto the CNT sidewalls during the oxidation treatment. These results clearly show that hydroxyl groups are introduced onto the surface of the h-SWCNTs, which is in good agreement with Ref. 18.

Next, our analysis was extended to characterization of field-induced stretching of h-SWCNTs in an RM solution. A homogeneous mixture of the RM and h-SWCNTs (2 wt. %) was coated onto the substrate with interdigitated electrodes, and field-induced stretching of SWCNTs was performed. The thickness of the coated film fabricated by a spin-coating and a brush-coating technique was around  $1\text{ }\mu\text{m}$  and  $1.5\text{ }\mu\text{m}$ , respectively. Figure 3 shows optical microscopic textures of the films fabricated by each coating method. It is interesting to notice that the same h-SWCNT/RM mixture shows different degrees of dispersion depending on the coating method used. As Fig. 3(a) clearly shows, the h-SWCNT rods dispersed in the mixture were re-aggregated by van der Waals interactions between them due to the centrifugal force exerted by spin coating, forming dot-like clusters. When the brush coating method was used, on the other hand, the h-SWCNTs were uniformly distributed throughout the region, forming line-like clusters, as shown in Fig. 3(b). Even though the orientation of the line-like h-SWCNT clusters deviated slightly from the brushing direction, the overall dispersion of the

h-SWCNT clusters was uniformly spaced. More particularly, large h-SWCNT clusters were observed in the spin-coated film, while smaller clusters were evident in the brush-coated samples. The average cluster size was calculated as  $\sim 28\text{ }\mu\text{m}$  and  $\sim 8\text{ }\mu\text{m}$  for the spin- and brush-coated samples, respectively.

In order to stretch the CNT cluster along the field direction, the applied electric field should be strong enough to overcome the van der Waals forces between each CNT.<sup>20</sup> In the present study, the different degrees of dispersion of h-SWCNTs clearly show distinct van der Waals interactions between them in the LC medium. Accordingly, a square wave voltage with 60 Hz frequency was applied to both samples to further investigate the field-induced behavior of the h-SWCNT clusters. The optical microscopic images shown in Fig. 4 show that the h-SWCNT clusters were stretched along the field direction in both films. In particular, when the electric field was applied to the spin-coated film, most of the h-SWCNT clusters remained unresponsive to the field due to the strong van der Waals force resulting from their large size. In contrast, when the electric field was applied to the brush-coated film, the smaller line-shaped h-SWCNT clusters, which were uniformly dispersed across the sample area with a relatively weak van der Waals force between them, began responding to the field at  $1\text{ V}/\mu\text{m}$  and stretched out along the electric field direction at  $4\text{ V}/\mu\text{m}$ . In a previous study, we found that the threshold for field-induced stretching was dependent on cluster length; when clusters were longer, a stronger electric field was required to induce stretching.<sup>19,21</sup> Our results shown in Fig. 4 correspond closely with these previous findings.

Continuing to investigate the field-induced reorientation of CNT clusters, we next observed the time-resolved characteristics of h-SWCNT clusters in the brush-coated sample. Figure 5 shows the time-dependent behavior of h-SWCNT clusters in response to an electric field of  $4\text{ V}/\mu\text{m}$  applied at 60 Hz. The smaller h-SWCNT clusters stretched out fully along the field direction within 30 s, as shown in Fig. 5 (top row). While previous studies have reported that the elastic stretching response of CNT clusters in an LC medium was around 1 s,<sup>20</sup> in the present study, it took a relatively longer time of 30 s perhaps due to the high viscosity of the UV-curable

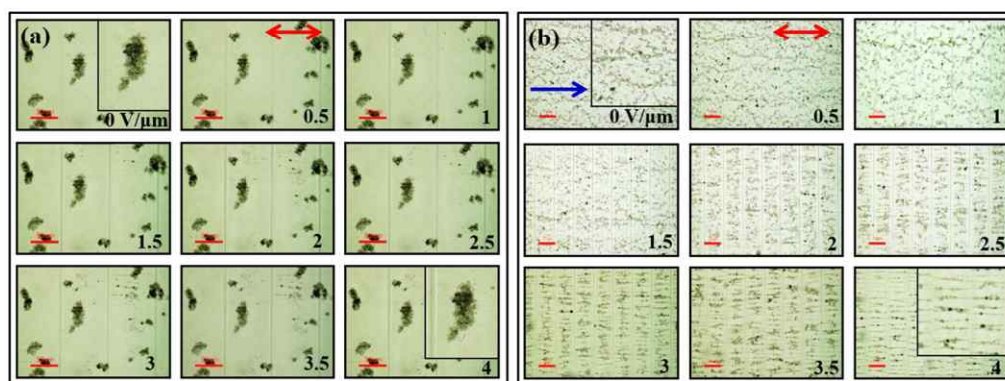


**FIG. 4.** Optical microscope images of the (a) spin-coated and (b) brush-coated sample as a function of electric field. Magnified images are shown in the inset. The red color double arrow indicates the applied field. The blue color arrow indicates the brushing direction.



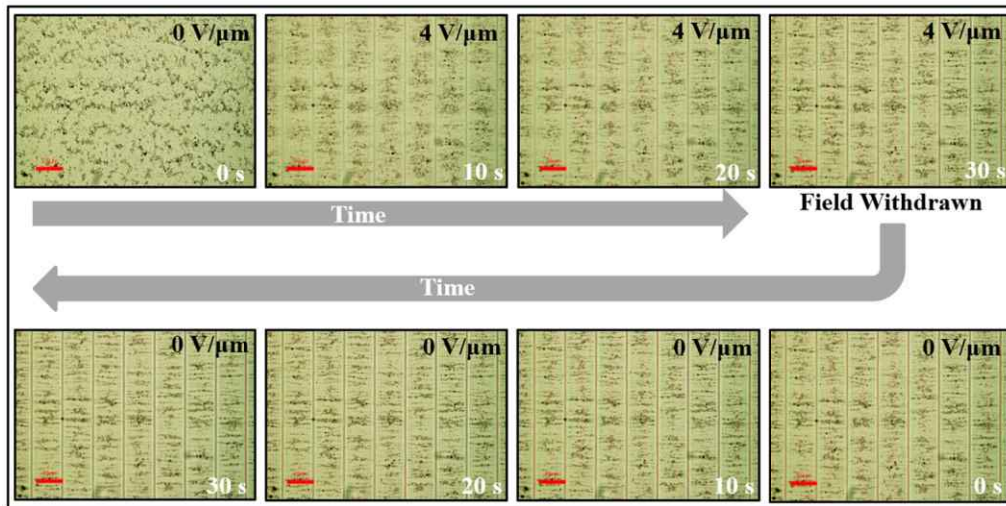


**FIG. 5.** Time-resolved optical microscopic images of h-SWCNT clusters in a thin film of the h-SWCNT/RM fabricated by brush coating. A field of  $4 \text{ V}/\mu\text{m}$  was applied for 30 s (top row) and then turned-off (bottom row).

RM-like gel. Once the SWCNT clusters had fully stretched out under the strong field, we withdrew the field and observed their relaxation mechanism. Very interestingly, the orientation ordering of the h-SWCNTs remained in the stretched position without resuming their initial state even after 30 s, as shown in Fig. 5 (bottom row). It can accordingly be assumed that the proposed approach is capable of producing efficient polarizers by tuning field-induced orientation to the structural properties of SWCNT clusters. These results suggest that the field  $4 \text{ V}/\mu\text{m}$  was sufficient to overcome the van der Waals forces within CNT clusters and to separate them into individuals or bundles with their long axis parallel to the field direction. After this, orientational ordering was preserved by the field of the high-viscosity RM.<sup>20,22</sup>

We further investigated the wavelength-dependent characteristics of the brush-coated polarizer by connecting it to a UV-visible spectroscope. Field-dependent transmittance properties were also measured as a function of polarization by supplying an appropriate electric field to the coated film. To avoid the possibility of polymerizing effects during the experiments, we set the incident light within the visible spectral range (i.e., not the UV-range). The polarization axis of the incident light was set either parallel ( $T_{\parallel}$ ) or perpendicular ( $T_{\perp}$ ) to the direction of the field applied, as shown in Fig. 6(a), and the transmitted light intensity was measured in a direction normal to the substrate. At the field-off state, as expected, both  $T_{\parallel}$  and  $T_{\perp}$  showed only minor differences since the SWCNTs in each cluster were not properly oriented. As the field

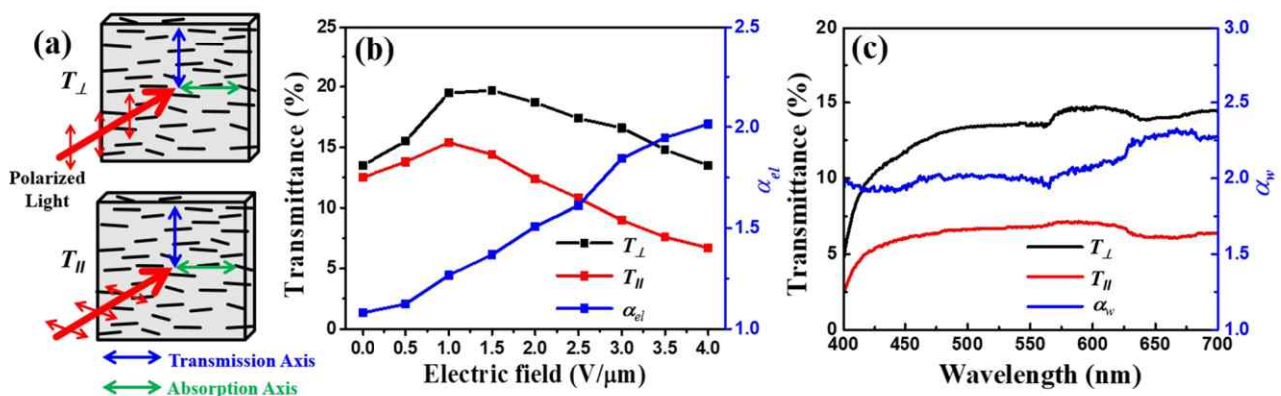


**FIG. 6.** (a) Schematic of  $T_{\perp}$  and  $T_{\parallel}$  of the brush-coated polarizer, (b) measured field-dependent  $T_{\perp}$ ,  $T_{\parallel}$ , and  $\alpha_{el}$ , and (c) wavelength-dependent  $T_{\perp}$ ,  $T_{\parallel}$ , and  $\alpha_w$  measured at a stretched state (at  $4 \text{ V}/\mu\text{m}$ ).



strength increased to  $1 \text{ V}/\mu\text{m}$ , however, the transmittance differences between the two became more noticeable and in both cases were higher than those without the electric field. As the field strength increased from  $1 \text{ V}/\mu\text{m}$  to  $4 \text{ V}/\mu\text{m}$ , the field-dependent extinction ratio ( $\alpha_{el}$ ), defined as  $T_{\perp}/T_{\parallel}$ , increased correspondingly from 1.08 to 2.01, as shown in Fig. 6(b). Surprisingly, the transmittance of both  $T_{\parallel}$  and  $T_{\perp}$  decreased as the electric field increased. An increase in  $T_{\perp}$  and a decrease in  $T_{\parallel}$  are to be expected as the electric field increases, if we assume that the orientation ordering of both individual and bundled CNTs becomes higher along the field direction as the electric field increases. The decrease in  $T_{\perp}$  is thought to be associated with the translational motion of stretched SWCNTs with increasing field strength, which disturbs their orientational ordering.<sup>23</sup> Figure 6(c) shows visible wavelength-dependent transmittance of the brush-coated film in its stretched state (at  $4 \text{ V}/\mu\text{m}$ ). Here, the average  $T_{\perp}$  and  $T_{\parallel}$  were found to be 14.5% and 6.5%, respectively. For its part, the wavelength-dependent extinction ratio,  $\alpha_w$ , remained unchanged, which means that the anisotropy in the absorption of SWCNTs was almost unchanged across the entire visible spectra. As with field-dependent transmittance, the wavelength-dependent transmittance results indicate that more visible light is absorbed when its electric vector propagates along the long axis of the stretched h-SWCNT aggregate than in the case when the electric field propagates along its short axis. The results indicate that differences in transmittance between  $T_{\parallel}$  and  $T_{\perp}$  of oriented h-SWCNT/RM films originate from the polarization selection rule related to the  $\pi$ - $\pi$  transition of electrons between the Van Hove singularity of the SWCNTs.<sup>13</sup>

Next, a narrow-band UV light with a center wavelength of 365 nm was irradiated onto the h-SWCNT/RM film in order to polymerize the RM so that the orientational ordering of stretched SWCNTs could be fixed in an RM polymer matrix. Here,  $T_{\parallel}$  and

$T_{\perp}$  were defined as the transmittance of incident polarized light when the polarization direction was either parallel or perpendicular, respectively, to the average orientation of the SWCNT. As shown in Fig. 7(a), the transmission spectra and corresponding optical microscopy images of the brush-coated samples exhibited a slight improvement in anisotropic absorption of the SWCNT after polymerization. In addition, the extinction ratio of the polarizer ( $\alpha_p$ ) after polymerization remained constant compared to the pre-polymerization spectra shown in Fig. 6(c). The inset optical-microscope images shown in Fig. 7(a) were obtained when the transmission axis of the polarizer remained parallel and perpendicular to the stretching direction of the h-SWCNT clusters. As is clearly evident, the stretched h-SWCNTs are visible mostly as dark lines in the microscope images of  $T_{\parallel}$ , while they become thinner, albeit not completely transparent, in the microscope images of  $T_{\perp}$ . This suggests that although the orientational degree of individual CNTs in a stretched cluster was perfectly aligned, some large clusters may not have stretched out well along the field direction, which would account for the low  $\alpha_p$  yield. Another noteworthy observation was that the transmittance of both  $T_{\parallel}$  and  $T_{\perp}$  was increased after polymerization, which preserves the orientational ordering of the stretched CNTs in smaller clusters via a translational motion by cross-linking RM molecules in a predefined direction. However, the polymerization processing seemed to slightly decrease  $\alpha_p$  while increasing transmittance, which followed the physical characteristics of a conventional iodine-type polarizer, in which the lower the degree of polarization (DOP), the higher the transmittance. The degree of polarization (DOP), defined as  $\{(T_{\perp} - T_{\parallel})/(T_{\perp} + T_{\parallel})\}^{1/2} \times 100\%$ , was calculated as  $\sim 37\%$ , as shown in Fig. 7(b). The small DOP is thought to be due to the low concentration of SWCNTs. Figure 7(c) shows the wavelength-dependent transmittance of a single h-SWCNT film fabricated without using a polarizer i.e.,

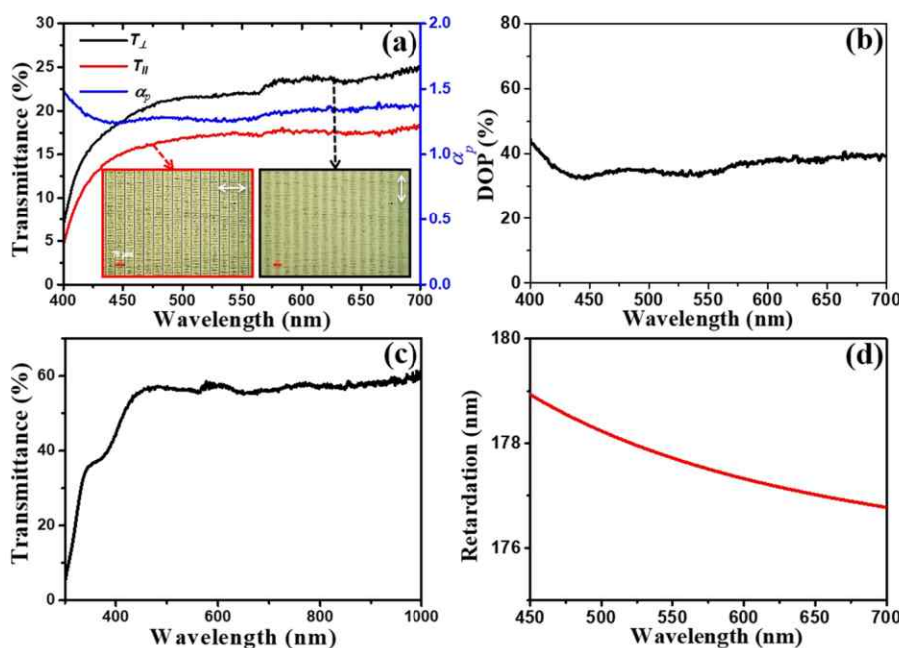


**FIG. 7.** (a) Measured transmittance of  $T_{\perp}$ ,  $T_{\parallel}$ , and  $\alpha_p$  as a function of visible wavelength and insets are optical microphotographs of the stretched CNT embedded in a liquid crystal polymer matrix when the polarized direction of incident light is parallel and perpendicular to the long axes of the stretched CNTs. The arrow on microscopic images indicates the transmission axis of the polarizer, (b) the calculated DOP after polymerization of the RM, (c) wavelength-dependent transmittance of fabricated polarizer. The incident light is unpolarized here, and (d) the measured retardation of the polarizer.



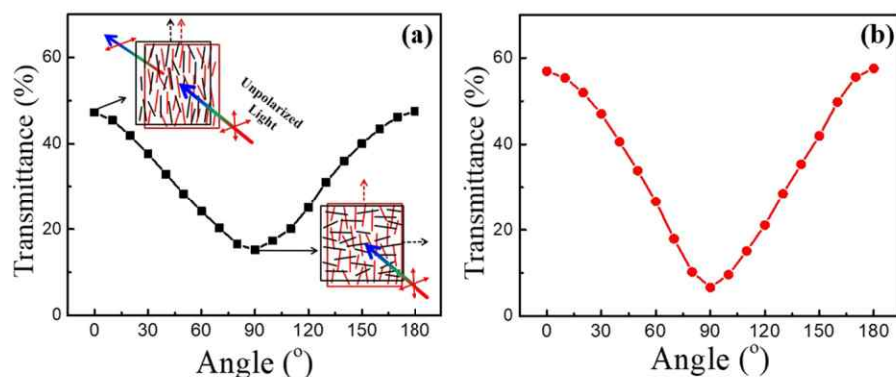


**FIG. 8.** Polarization efficiency of the prepared coatable polarizer: (a) spin-coating and (b) brush-coating. The measurement scheme is shown in the inset. Dotted arrows indicate the absorption axis of the respective polarizer. The solid double arrows indicate the polarization direction of the transmitted light.

unpolarized light. As shown in Fig. 7(c), the film was capable of extending the attenuation of incident light in the UV region (the transmittance of a conventional iodine polarizer below 400 nm was almost zero) while providing a wider operating wavelength range from 300 nm to 700 nm, suggesting that the proposed polarizer can work in the UV region as well. The alignment of RM molecules was also confirmed by measuring the retardation value of the film by using REMS-150 (Sesim Photonics Technology). The finite retardation value, shown in Fig. 7(d), indicates that the RM molecules are aligned along the electric field direction so that the polymerized film may create an optic axis. In other words, as a result of the combined effect of the RM and the SWCNT, the film acts both as an optical polarizer from the UV to visible wavelength and as an optical birefringent film.

In a final step, the efficiency of the two coatable polarizers was examined by rotating them while positioned above one another and measuring the resulting transmitted light. Unpolarized white light was used as the light source. The upper polarizer was fixed, while the lower one was rotated from  $0^\circ$  to  $180^\circ$ . As seen in Fig. 8, the two polarizers exhibited maximum transmittance when parallel to one another. Furthermore, the light transmittance decreases with an increase in the polarizer's rotation angle and achieved minimum transmittance when the two polarizers are crossed, i.e.,  $90^\circ$  to each other. In other words, polarized light transmitted from the upper polarizer was mostly absorbed by the lower one, thereby reducing transmission to a minimum. In both cases, the transmitted light is found to be a linearly polarized light in a direction perpendicular to the average orientation of the SWCNT. However, when the polarizers crossed, the brush-coated polarizer effectively absorbs most of the incident light [Fig. 8(b)], whereas the spin-coated polarizer emitted feeble light even in a direction normal to the polarizers [Fig. 8(a)]. Field-induced stretching of SWCNT clusters attained a high degree of relative orientation after the polarization of the RM in the brush-coating method, which is effective in absorbing incident light. Not only does the brush-coated polarizer act as an efficient birefringent polarizer but it also has the advantages of ease of manufacture coupled with reduced device costs and large-area displays.

#### IV. CONCLUSION

We have demonstrated here an optical polarizing CNT film in which a solution of short-length CNTs and an RM is brush-coated

onto a substrate, after which an electric field assists in stretching out the CNT clusters and aligning their long axes and the RM with the field direction. The solution is polymerized by UV irradiation, fixing the orientational ordering of the stretched CNTs and the RM. The h-SWCNT polarizer fabricated using a brush-coating method shows a highly uniform dispersion of the CNT over a large area compared to that fabricated using the conventional spin-coating method, which makes field-induced stretching possible. Very interestingly, the optical film composed of stretched h-SWCNTs shows selective anisotropic light absorption properties, from UV to visible light, and birefringence, enabling it to act both as a polarizer and an optical film. While the brush-coating method for fabricating h-SWCNT polarizers confirms the feasibility of a broadband film polarizer that can be applied to flexible displays, substantial future improvements in its degree of polarization are nevertheless still required.

#### ACKNOWLEDGMENTS

This work was supported by the Innovation Lab support program for material, parts, equipments (20012555, Commercialization of nanocarbon composites materials in electric and electronic display and energy industries) funded by the Ministry of Trade, Industry & Energy (MOTIE, Korea) and the research funds of Jeonbuk National University in 2019. W.T. also thanks the National Natural Science Foundation of China (Grant No. 6160516).

#### DATA AVAILABILITY

The data that support the findings of this study are available from the corresponding author upon reasonable request.

#### REFERENCES

- 1 E. H. Land, *J. Opt. Soc. Am.* **41**, 957 (1951).
- 2 R. Manda, S. Pagidi, Y. J. Lim, R. He, S. M. Song, J. H. Lee, G.-D. Lee, and S. H. Lee, *J. Mol. Liq.* **291**, 111314 (2019).
- 3 G. Tan, J.-H. Lee, Y.-H. Lan, M.-K. Wei, L.-H. Peng, I.-C. Cheng, and S.-T. Wu, *Optica* **4**, 678 (2017).
- 4 P. Im, Y.-J. Choi, W.-J. Yoon, D.-G. Kang, M. Park, D.-Y. Kim, C.-R. Lee, S. Yang, J.-H. Lee, and K.-U. Jeong, *Sci. Rep.* **6**, 36472 (2016).
- 5 E. Chang, J. K. Cho, and S. Shin, *Prog. Org. Coat.* **85**, 38 (2015).
- 6 S.-K. Park, S.-E. Kim, D.-Y. Kim, S.-W. Kang, S. Shin, S.-W. Kuo, S.-H. Hwang, S. H. Lee, M.-H. Lee, and K.-U. Jeong, *Adv. Funct. Mater.* **21**, 2129 (2011).



- <sup>7</sup>T. Ikeda, *J. Mater. Chem.* **13**, 2037 (2003).
- <sup>8</sup>K. Ichimura, *Chem. Rev.* **100**, 1847 (2000).
- <sup>9</sup>M. Schadt, K. Schmitt, V. Kozinkov, and V. Chigrinov, *Jpn. J. Appl. Phys., Part I* **31**, 2155 (1992).
- <sup>10</sup>C.-T. Wang and T.-H. Lin, *Opt. Mater. Express* **1**, 1457 (2011).
- <sup>11</sup>Y.-H. Lin, J.-M. Yang, Y.-R. Lin, S.-C. Jeng, and C.-C. Liao, *Opt. Express* **16**, 1777 (2008).
- <sup>12</sup>J. B. Chang, J. H. Hwang, J. S. Park, and J. P. Kim, *Dyes Pigm.* **88**, 366 (2011).
- <sup>13</sup>S. Shoji, H. Suzuki, R. P. Zaccaria, Z. Sekkat, and S. Kawata, *Phys. Rev. B* **77**, 153407 (2008).
- <sup>14</sup>L. Ren, C. L. Pint, L. G. Booshehri, W. D. Rice, X. Wang, D. J. Hilton, K. Takeya, I. Kawayama, M. Tonouchi, R. H. Hauge, and J. Kono, *Nano Lett.* **9**, 2610 (2009).
- <sup>15</sup>B. G. Kang, Y. J. Lim, K.-U. Jeong, K. Lee, Y. H. Lee, and S. H. Lee, *Nanotechnology* **21**, 405202 (2010).
- <sup>16</sup>W. Tie, S. S. Bhattacharyya, Z. Xheng, K. J. Cho, T. H. Kim, Y. J. Lim, and S. H. Lee, *Liq. Cryst.* **47**, 317 (2020).
- <sup>17</sup>Y. Xing, L. Li, C. C. Chusuei, and R. V. Hull, *Langmuir* **21**, 4185 (2005).
- <sup>18</sup>F. Avilés, J. V. Cauch-Rodríguez, L. Moo-Tah, A. May-Pat, and R. Vargas-Coronado, *Carbon* **47**, 2970 (2009).
- <sup>19</sup>S. S. Bhattacharyya, G. H. Yang, W. Tie, Y. H. Lee, and S. H. Lee, *Phys. Chem. Chem. Phys.* **13**, 20435 (2011).
- <sup>20</sup>S. J. Jeong, K. A. Park, S. H. Jeong, H. J. Jeong, K. H. An, C. W. Nah, D. Pribat, S. H. Lee, and Y. H. Lee, *Nano Lett.* **7**, 2178 (2007).
- <sup>21</sup>W. Tie, S. S. Bhattacharyya, H. R. Park, J. H. Lee, S. W. Lee, T. H. Lee, Y. H. Lee, and S. H. Lee, *Phys. Rev. E* **90**, 012508 (2014).
- <sup>22</sup>W. Tie, G. H. Yang, S. S. Bhattacharyya, Y. H. Lee, and S. H. Lee, *J. Phys. Chem. C* **115**, 21652 (2011).
- <sup>23</sup>I.-S. Baik, S. Y. Jeon, S. J. Jeong, S. H. Lee, K. H. An, S. H. Jeong, and Y. H. Lee, *J. Appl. Phys.* **100**, 074306 (2006).